Neutron Pendellösung Fringe Structure in the Laue Diffraction by Germanium *

C. G. Shull and W. M. Shaw

Massachusetts Institute of Technology, Cambridge, Massachusetts, USA

(Z. Naturforsch. **28 a**, 657–661 [1973]; received 22 January 1973)

Dedicated to Gerhard Borrmann on his 65th birthday

The Pendellösung fringe structure within the Bragg reflection from perfect crystals of germanium has been studied over a wide interference range using full-spectrum incident neutron radiation. After allowing for the effects of residual crystal curvature, the experimental data yield a precision determination of the crystal structure amplitude. The coherent nuclear scattering amplitude for germanium is determined to be $0.81858(36) \times 10^{-12}$ cm.

Introduction

In recent years it has been established in a series of studies that the Pendellösung fringe structure within the Bragg beam reflected from perfect crystals is capable of providing very precise information on crystal structure factors. These studies have been performed with both X-rays and neutrons and, although the most effective exploitation of the method requires different techniques for the two cases, it has been demonstrated that a precision of one part in about 5000 is attainable in the determination of the crystal structure factor. Since the method depends fundamentally on geometrical measurements, of length and angle, and only secondarily on intensity measurement, the ultimate precision is limited only by the care of the experimentalist in determining these quantities and by the source intensity. The latter arises because it controls the geometrical resolution of the system under study consistent with having measurable intensity. The attainment of high precision is of interest because it can provide information on very small and subtile contributing factors to the absolute structure factor, such as electron bonding and anomalous temperature motion in the X-ray case and on some of the non-nuclear scattering contributions in the neutron case.

In the present report we summarize the results of Pendellösung fringe studies made with neutron radiation on a series of Ge crystals. They represent an extension of an earlier study [1] performed with the same technique on Si crystals. Taken together these studies have provided neutron technologists with standard nuclear scattering amplitudes of much higher precision than has been possible from diffraction intensity methods.

* Research supported by the National Science Foundation, Washington, D.C., U.S.A.

Reprint requests to Dr. C. G. Shull, Massachusetts Institute of Technology, *Cambridge*, Massachusetts 02139, U.S.A.

Experimental Techniques

The experiments have been performed with parallel-faced slices of low-dislocation density, perfect crystals of Ge. A one-axis neutron spectrometer has been used in which the white, full-spectrum neutron radiation from a nuclear reactor is introduced to the crystal through a fine slit opening as illustrated in Figure 1. The crystal slice is cut and oriented so

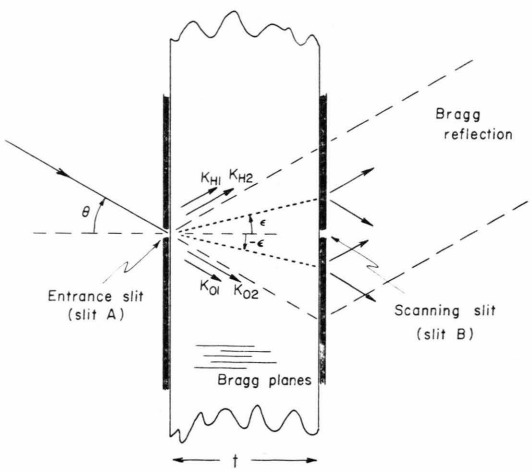

Fig. 1. Diagram of experimental arrangement for studying Plendellösung fringe structure within the Bragg reflection from a Laue transmitting crystal. Full spectrum incident neutron radiation is used in the experiment.

that the diffracting (111) planes are accurately perpendicular (within 1 minute arc) to the entrance face and thus the crystal is arrayed in symmetrical Laue transmission. A second slit opening is positioned on the exit face of the crystal along the net planes from the entrance slit opening and an open detector

responds to all of the Bragg reflected intensity emanating through the exit slit opening.

With white radiation falling on the crystal, a band of wavelengths will be diffracted by the perfect crystal with the band width being determined by the entrance beam collimation. In the present experiments the incident beam was collimated by a converging, non-reflecting surface collimator of angular width 3 minutes. High collimation is necessary to maintain fringe contrast which will suffer if the wavelength band width is too large as discussed later. Rotation of the crystal and its associated slit openings will, of course, change the Bragg angle for diffraction and the full range of wavelengths in the spectrum can be scanned consistent with measurable intensity limitations. The fringe pattern arises as a periodic modulation of the intensity as the spectrum is scanned. It should be mentioned that germanium exhibits, like silicon, very little true absorption for neutron radiation so that all of the wave fields indicated in Fig. 1 are fully excited with only minimal Borrmann action occurring.

Three crystal slices of Ge of different thickness, ranging from approximately 2.4 to 6.5 mm, have been used in the study. The crystal slices were cut with a diamond-imbedded saw, mechanically polished with successively finer abrasive, and finally chemically polished to remove the surface mosaic layer. The various stages of polishing were performed with apparatus designed to maintain proper orientation and parallelness of the entrance and exit faces. Because of its high absorptivity for neutron radiation, gadolinium metal was used as the slit limiting material with the edges being taper ground at an angle of 15°. Slit openings of 0.12 mm width and 10 mm length were fabricated under microscope observation with care being taken to maintain parallelness of the edges. Because the opacity of gadolinium metal varies with neutron wavelength, the effective width of the slit opening changes slightly as the spectrum is scanned. This in turn causes a small shift in the fringe position necessitating a small correction to the data which will be discussed later.

In the fringe measurement it is necessary to have the two slit openings positioned accurately along common net planes and aligned parallel to each other. This was accomplished with a micrometer system which could tip and position one slit opening relative to the other. The central positioning of the exit slit was determined by translating it across the full width Bragg beam with the Kato profile edges being used to determine the central location. In scanning over the spectrum, rotation of the crystal-slit system was performed with the entrance slit opening centered on the rotation axis. Since only a very small fraction of the incident intensity is selected by the crystal for diffraction, judicious shielding between the exit slit opening and the detector is called for in order to reduce background intensity arising from incoherent scattering. This was accomplished with a diverging collimator leading radiation to the detector and directed at the exit slit opening, with its angular motion synchronized with the crystal motion. Care was taken that this collimator accepted all of the coherent Bragg intensity released through the exit slit opening.

Experimental Results

Full spectrum fringe patterns have been taken for three Ge crystals, labelled A, B and C, by observing the intensity modulation as the crystal is rotated slowly relative to the incident beam direction. Because there exists complete symmetry for scattering to the left and to the right relative to the incident beam direction in this one-axis spectrometer mode, patterns can be taken on both sides and then matched with each other. The left-right fringe matching was accomplished without trouble by wavelength matching since there is a singular correlation between wavelength and fringe order. Data collection on both sides obviously improves the precision of the fringe positions, since it permits averaging angular scale irregularities over a larger angular range, as well as eliminating the need for establishing the incident beam direction.

Figure 2 illustrates small portions of the fringe patterns obtained for crystals A and B in which the diffracted intensity is displayed as a function of the angular position of the crystal. The fringe order numbers, to be defined later, are shown on the figure as well as calculated wavelength positions. In spite of the rather low intensity (with statistical uncertainty) and modest contrast (because of incoherent background scattering) the angular positions of the fringe maxima-minima can be well established. The fringe patterns were collected to either end of the spectrum as limited by meaningful data collection. In practice the useful fringe modulation range extended between wavelengths 0.70 to 1.74 Å with fringe order values ranging from 14 to 94 for the crystal thickness values that were studied. There is of course a variation of the mean modulated intensity and of the incoherent background across the spectrum, and in principle this implies a small shift

in the fringe positions. This was considered in assessing the experimental fringe positions from the graphical display. A number of wavelength dependent factors contribute to this intensity variation across the spectrum including the incident beam spectrum, the crystal reflectivity, the wavelength band width, the detector efficiency and the incoherent intensity. Aside from the general, long-range intensity envelope affecting the fringe intensity no other intensity perturbations were recognizable across the spectrum.

After collecting and matching the left and right side fringe patterns, the crystal angular positions corresponding to the various left-right maxima and minima were tabulated. By taking half of the sum of any matched pair of values one obtains the angular position of the diffracting net planes and these values showed remarkable consistency across the fringe patterns. For instance the standard error associated with the variations from the mean value of this quantity for the case of crystal A, where 116 fiducial positions were available, was found to be 0.024 minutes arc. No significant trend in the variations from the mean were discernible across the spectrum and this implies that angular scale irregularities were beyond observation. In collecting data on both sides of the incident beam, the scanning was performed always in one direction thereby eliminating spectrometer backlash effects. Alternatively the difference between matched left-right angular positions yields twice the Bragg angle θ_n at which the maxima-minima occur. The corresponding neutron wavelength values were than available from the unit cell dimensions.

Interpretation of Results

As in the case of an earlier study on the Pendellösung fringe structure in silicon, spherical wave theory is expected to be satisfied [1, 2] by the conditions of the present experiments. Kato [3] has shown for this case that the modulated fringe intensity I should be given by

$$I = C(1-\gamma^2)^{-1/2} J_0^2(A[1-\gamma^2]^{1/2}\tan\theta) \qquad (1)$$

with

$$A = 2\,t_0 N\,\mathrm{d}\,(F_{\mathrm{H}} F_{\overline{\mathrm{H}}})^{1/2},$$
$$\gamma = \tan\varepsilon/\tan\theta\,.$$

J_0 is the Bessel function of zero order, t_0 the crystal thickness, N the unit cell density, F_{H} the crystal structure amplitude per unit cell, d the interplanar spacing and ε is the angular positions of the exit slit opening with respect to the entrance slit as measured relative to the net planes (see Figure 1). For all of the present experimental observations, the asymptotic form of the Bessel function can be used with sufficient precision to yield

$$I = C(1-\gamma^2)^{-1/2}\sin^2(\tfrac{1}{4}\pi + A[1-\gamma^2]^{1/2}\tan\theta)\,. \qquad (2)$$

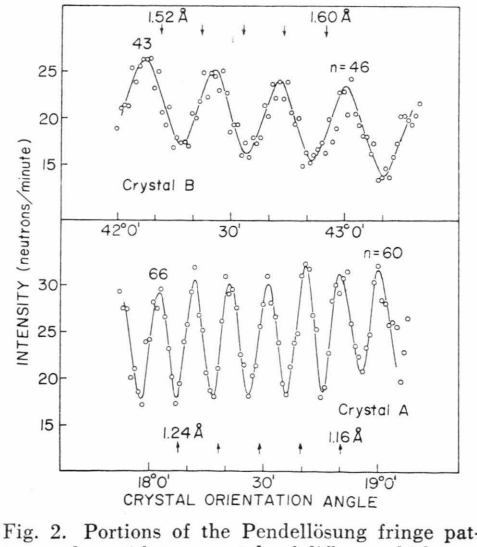

Fig. 2. Portions of the Pendellösung fringe patterns taken with two crystals of different thickness. Fringe order numbers are shown along with fiducial neutron wavelength positions.

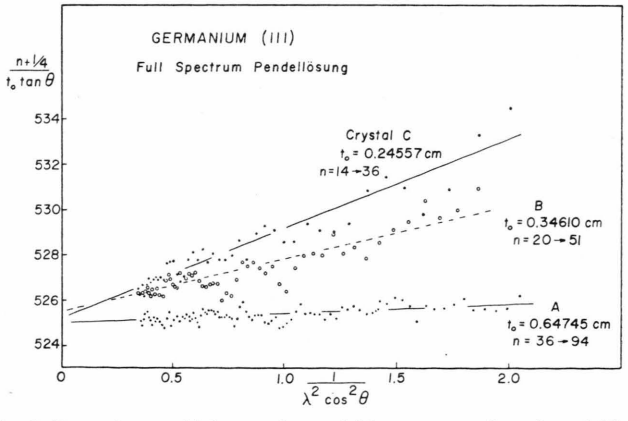

Fig. 3. Dependence of fringe order variable upon wavelength variable $(\lambda\cos\theta)^{-2}$. Uniform crystal curvature should result in a linear dependence with a common intercept for crystals of different thickness. The intercept depends upon the crystal structure amplitude and the slope is a measure of the crystal curvature.

Table 1. Germanium Pendellösung Fringe Results.

Crystal	Thickness (cm)	Fringe Order Range	Radius of Curvature (m)	$b\,e^{-W}$ (10^{-12} cm/atom)
A	0.64745(10)	36 → 94	18280	0.80813(14)
B	0.34610(3)	20 → 51	4050	0.80856(20)
C	0.24557(10)	14 → 36	2200	0.80854(42)
	Weighted mean $b\,e^{-W}=0.80829(15)$			

Thus the intensity is expected to be periodic in the variable $\tan\theta$. Defining n as the order of interference of a fringe maximum, Eq. (2) predicts that the quantity $(n+1/4)/t_0\tan\theta_n$, called the fringe order variable, should be constant over the full spectrum for all crystal-thickness values and this constant serves to establish the crystal structure amplitude.

Before discussing the relationship between the experimental results and the theoretical formulation, it is necessary to consider a correction that must be applied to the experimentally determined values of $\tan\theta_n$.

Equation (2) includes in the argument of the periodic term the quantity $(1-\gamma^2)^{1/2}$. As mentioned earlier, the experiment is performed with the exit slit opening being carefully positioned along common net planes relative to the entrance slit opening and hence $\gamma=0$. However, this is true only on the average and because of the quadratic form of the term $(1-\gamma^2)^{1/2}$, this term is not strictly of unit value for the case of finite slit openings. This results in a small shift in the observed fringe positions from those that would be measured under ideal conditions, and moreover this shift varies across the spectrum. The magnitude of this correction was evaluated for each crystal thickness value across the spectrum by computer integration over the angle ε, with inclusion of a triangular ray density factor characteristic of ray passage through two equivalent slits, to limits determined by the slit width. Moreover the limit of integration was variable across the spectrum because of intensity seepage through the tapered slit edges as discussed earlier. At most this correction amounted to about 10 percent of the fringe periodicity for the case of the thinnest crystal at the short wavelength end of the spectrum and it became negligible for the thickest crystal with long wavelength fringes. In this way, a corrected set of values of $\tan\theta_n$ were obtained which should be represented by Eq. (2) with $\gamma=0$.

With these corrected $\tan\theta_n$ values, it was found that the fringe order variable $(n+1/4)/t_0\tan\theta_n$ was not constant across the spectrum, as expected from Eq. (2), but rather it varied in a regular way much outside of experimental uncertainty. A similar effect had been found in the earlier study on silicon where it was found to arise from the effect of residual crystal curvature. With crystal distortion in the form of uniform curvature of radius R, Kato [4] has shown that an additional wavelength dependence is introduced into the argument of the periodic term of Eq. (2) so that it becomes

$$I = C'\sin^2[\pi/4 + A f(p)\tan\theta],$$

$$\text{with}\quad f(p) = \tfrac{1}{2}\left[(1+p^2)^{1/2} + p^{-1}\ \text{invsinh}\,p\right] \qquad (3)$$

$$= 1 + p^2/6 - p^4/40 + p^6/116 + \ldots,$$

$$p = \pi t_0^2/R\lambda A\cos\theta.$$

This functional form predicts in first approximation with inclusion of p^2 terms, that the fringe order variable should show a linear dependence upon the variable $(\lambda\cos\theta_n)^{-2}$ with extrapolated intercept being dependent upon the quantity A or F_H and with slope value being dependent upon the crystal radius of curvature R. Figure 3 shows the expected linearity for the fringe spectra obtained for the three crystals that were studied. The straight lines extrapolate to a common intersection at infinite wavelength and the different slopes imply different curvature distortion in the crystals as they were examined. The straight lines in the figure are least squares fitted to the data points and illustrate the general quadratic dependence. However, for the final extraction of the parameter values, higher order terms were included in the analysis, which is simplified materially by recognition that

$$f(p) = (1+7p^2/15)^{5/14}$$

to sixth order.

From the fringe data fitting illustrated in Fig. 3, the parameters A and R are obtained for each case. Finally using precision thickness values [5] which were obtained for the crystal slices and the unit cell dimension [6] for germanium $a_0=5.6575$ Å, the quantity $b\,e^{-W}$ is determined with b being the atomic scattering amplitude and e^{-W} being the Debye-Waller temperature factor. These results are collected in Table 1 for the three cases with the parenthesized numbers being the standard errors in the last digits of the quantities. It is to be noted that the curvature distortion is very small, with very

large curvature radius, in spite of the rather pronounced slope of the fitted lines in Figure 3. This demonstrates the extreme sensitivity of the fringe pattern to crystal distortion. The weighted mean value for the effective atomic scattering amplitude $b\,e^{-W}$ becomes $0.80829(15)\times10^{-12}$ cm with the standard error (15 units) being determined from the variations from the mean. From the precision of the individual values, one would expect a standard error of 11 units for the mean on the basis of random statistical variations of the three entries. Using the larger error it is seen that the crystal structure amplitude is determined to a precision of about one part in 5000.

In extracting the true atomic scattering amplitude from the above, the Debye-Waller factor must be utilized. Batterman and Chipman [7] have reported a value for the Debye characteristic temperature of 290(5) °K from careful X-ray intensity measurements and this leads to $e^{-W}=0.9867(4)$ for the (111) reflection at our ambient temperature of 295 °K. Thus the germanium atomic scattering amplitude becomes $0.81919(36)\times10^{-12}$ cm with somewhat reduced precision because of uncertainty in the temperature factor. Finally, this atomic scattering amplitude has two components arising from (1) the pure nuclear force interaction and (2) the Foldy charge scattering. For the latter contribution, the most recent experimentally determined interaction strength leads to an atomic amplitude of $+0.00061\times10^{-12}$ cm for the present case. Thus the coherent nuclear scattering amplitude for germanium becomes $0.81858(36)\times10^{-12}$ cm. At the present time there is no other value of significant precision for comparison with the fringe result. Earlier Bragg intensity measurements had yielded the value $0.84(2)\times10^{-12}$ cm which is not inconsistent with the present value.

[1] C. G. Shull and J. A. Oberteuffer, Phys. Rev. Letters **29**, 871 [1972].
[2] C. G. Shull, General Lecture presented at Ninth International Congress of Crystallography, Kyoto, Japan, August 1972, to be published J. Appl. Cryst. and Jap. J. Cryst.
[3] N. Kato, Acta Cryst. **14**, 526 [1961] and **14**, 627 [1961].
[4] N. Kato, J. Phys. Soc. Japan **19**, 971 [1964].
[5] The thickness was established by intercomparison with standard gage blocks with an electric-sensing instrument. A survey was made over regions of the crystal illuminated by the neutron beam and the standard errors in Table I arise from the variations in measurement.
[6] International Table for X-ray Crystallography, Vol. III, The Kynoch Press, 1962.
[7] B. W. Batterman and D. R. Chipman, Phys. Rev. **127**, 690 [1962].

Electron and Positron Density Distribution of Bloch Waves *

G. Lehmpfuhl

Fritz-Haber-Institut der Max-Planck-Gesellschaft, Berlin-Dahlem *

(Z. Naturforsch. **28** a, 1 [1973]; received 24 October 1972)

Dedicated to Professor Dr. G. Borrmann on his 65th birthday

The charge density distribution in the strongest Bloch waves for a dynamical many-beam diffraction situation was calculated for electrons and positrons. Near the [110] zone axis of MgO there exist three strong Bloch waves for electrons. One Bloch wave is concentrated at the rows of Mg-atoms, a second at the rows of O-atoms and a third one between the atoms. The positron Bloch waves are mainly concentrated between the atom rows and have only small charge density at the positions of the atoms. For an incident beam parallel to the [110] axis there exists only one strong positron Bloch wave while for electrons more than three Bloch waves are strong, explaining the channeling behaviour of positrons and electrons. Strong partial waves of different electron Bloch waves can be identified in the diffraction pattern from a MgO crystal wedge.

* Siehe Z. Naturforsch. Heft 1.
** Abteilung Prof. Dr. K. Molière.